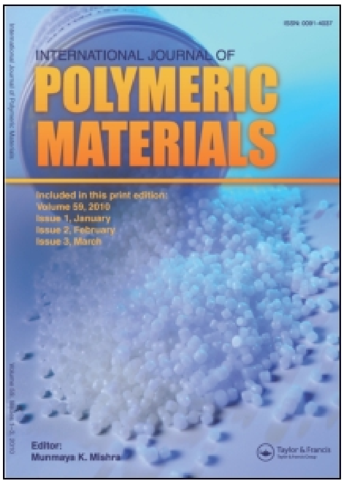

International Journal of Polymeric Materials
Publication details, including instructions for authors and subscription information:
http://www.informaworld.com/smpp/title~content=t713647664

Application of Upper Bound Theory to Solid-State Extrusion of Polymers

S. Maruyama[a,b]; K. Imada[a]; M. Takayanagi[a]
[a] Faculty of Engineering, Kyushu University, Fukuoka, Japan [b] Mitsubishi Chemical Ind. Co., Ltd.,

To cite this Article Maruyama, S. , Imada, K. and Takayanagi, M.(1973) 'Application of Upper Bound Theory to Solid-State Extrusion of Polymers', International Journal of Polymeric Materials, 2: 2, 125 — 136
To link to this Article: DOI: 10.1080/00914037308075304
URL: http://dx.doi.org/10.1080/00914037308075304

Intern. J. Polymeric Mater., 1973, Vol. 2, pp. 125–136

Printed in Great Britain

Application of Upper Bound Theory to Solid-State Extrusion of Polymers

S. MARUYAMA,† K. IMADA and M. TAKAYANAGI
Faculty of Engineering, Kyushu University, Fukuoka, Japan

(*Received October* 26, 1972)

Solid-state extrusion of some crystalline polymers, such as high density polyethylene, isotactic polypropylene and nylon 6, were analyzed on the basis of the upper bound theorem. The method of practical application of the theorem was the same as that described by Avitzur, and an improvement was added by taking into account of the strain hardening effect of the polymeric materials. The agreement between calculated and observed results was fairly good with the frictional coefficient of the values coincident with those estimated in previous papers with the other approach. And the cause of the increase of the extrusion pressure with increasing die taper angle was confirmed as due to the discontinuous change of the velocity distributions, especially around the exit of the die.

1 INTRODUCTION

Solid-state extrusion of polymeric materials was investigated from the view-points of superstructures,[1] and analyzed according to the pressure balanced schema of Sachs and also by slip-line analysis.[2] Those treatments revealed the plastic nature of crystalline polymers and gave a fair prospect of the extrusion process. In the present paper we will describe the application of the upper bound theorem to analyze the solid-state extrusion process of polymeric materials. The analysis starts from the assumption of velocity field within the die. If the energy is as low as was expected, the velocity field assumed is admitted to be a reasonable one. As mentioned in a previous paper,[2] slip-line analysis gives an estimation of velocity field within the die of hypothetical

† Visiting research fellow from the Mitsubishi Chemical Ind. Co., Ltd.

plane extrusion. An extended Sachs equation[2] gives a good estimation of extrusion pressure without assuming any velocity distributions. The method of the upper bound theorem will be useful to examine the adequateness of both methods. In the present paper we will try to examine the applicability of the theorem according to the method described by Avitzur.[4] An improvement is introduced to extend the practical method so as to make it applicable for polymeric materials which shows remarkable strain-hardening effect in the high strain region.

2 EQUATION OF EXTRUSION PRESSURE

2.1 Stress–strain property of crystalline polymers

The flow curve, i.e. true stress–true strain curve determined by tensile testing, is the most convenient and useful measure of the strain-hardening effect of the material. Eq. (1) was found being a generalized expression of the true-stress and true strain relationship of crystalline polymers such as high density polyethylene, isotactic polypropylene, or nylon 6.[3]

$$\log(\sigma/\sigma^*) \cdot \log(\epsilon/\epsilon^*) = -c \tag{1}$$

where $c = 0.384, 0.23$ and 0.175 for polyethylene, polypropylene, and nylon 6, respectively. The values of the shift factors of σ^* and ϵ^* depend on the condition such as the temperature, the speed of extension and the grade or composition of the polymer. Eq. (1) represents the characteristics of the crystalline polymers that the stress grows steeply with the increase of the strain as large as ϵ^*. The increasing stress grows tending to infinity when the strain attains to a finite value of ϵ^* .Table I gives the parameters c, σ^*, and ϵ^* of some polymers, which will be needed in the following analyses.

2.2 Sachs type equation of extrusion pressure based on the equilibrium of forces[2]

Imada *et al.* has given the equation of the extrusion pressure, Eq. (2), on the basis of the pressure balance schema proposed by Sachs and by taking account of the strain-hardening of the flow curve of polymeric materials.

$$P_o = -(1 + B)\int_o^{\epsilon_f} \sigma(\epsilon)\exp(B\epsilon)d\epsilon + \left(\frac{R_o}{R_f}\right)^{2B} P(\epsilon_f) \tag{2}$$

Where $\epsilon = 2ln(R_o/R_f)$; R_o, R_f are the inlet and outlet radii of the die respectively; P_o is the pressure at the die inlet, i.e. extrusion pressure, $P(\epsilon_f)$ the pressure at the die outlet, $\sigma(\epsilon)$ is the yield stress of the uniaxial tensile testing

TABLE I

Polymers used in extrusion experiments and their stress–strain characteristics

Polymers	Grade names	Stress–strain parameters[a]			
		temperature	c	σ^*	ϵ^*
High density polyethylene	Hizex 1200J[1]	30°C	0.384	1.28	5.75
		50	0.384	0.84	5.33
		90	0.384	0.46	5.55
		110	0.384	0.27	5.58
	Sholex 4002B[2]	90	0.384	0.41	4.82
	Novatec JVO40[3]	50	0.384	0.80	5.55
Isotactic polypropylene	Sumitomo-Noblen D501[4]	40	0.23	1.55	3.10
		70	0.23	1.00	3.50
Nylon 6	Amilan CM1031[5]	80	0.175	1.37	1.70
		120	0.175	1.26	1.78
		160	0.175	0.89	1.76

[a] Parameters c, σ^* and ϵ^* are the same as in Eq. (1). Extension speed 5 mm/min.
[1] Mitsui Petrochemical Co., Melt Index (M.I.) = 9.2.
[2] Nihon Olefin Co., M.I. = 0.2, (Copolymer with butene-1).
[3] Misubishi Chemical Co., M.I. = 4.0.
[4] Sumitomo Chemical Co., M.I. = 0.3.
[5] Toray Co.

at the strain ϵ, and $B = \mu \cot \alpha$; μ the coefficient of friction between the material and the inner surface of the steel die, and α the taper angle of the die. We assume the value of $P(\epsilon_f) = 0$.

2.3 Application of upper bound theorem for extrusion through conical converging die

2.3.1 *Extrusion pressure estimation without assuming the formation of dead zone* Avitzur[4] gave detailed descriptions of the practical method of applying the theorem originally established by Prager and Hodges.[5] In the following paragraphs we will apply the theorem according to Avitzur's method. An improvement was needed to apply the method to polymeric materials. The extrusion of crystalline polymers was conducted successfully with high degree of processing, i.e. with large decrement of cross sectional area before and after the extrusion. As mentioned in the preceding paragraphs, stress grows steeply in the region of high strain tending to infinity. Thus, the yield stress, which was considered to be constant over the whole range of deformation in Avitzur's treatment of metal extrusion, shall be regarded as a function of strain. Figure 1 is the figure showing the assumed velocity field

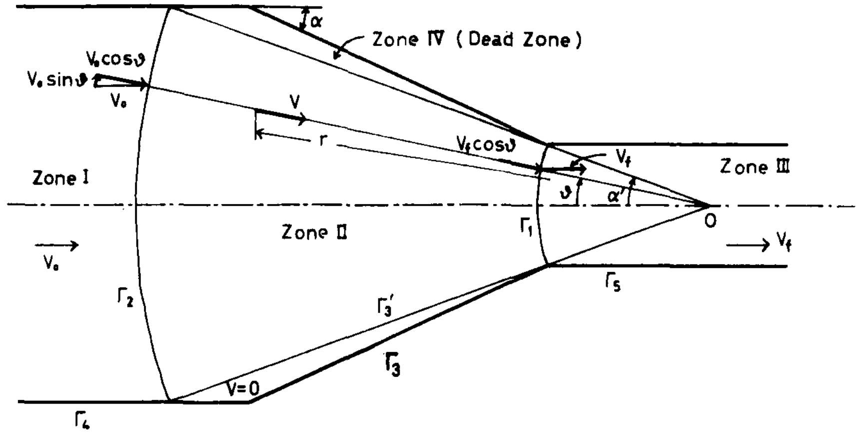

FIGURE 1 Longitudinal section of conical die and assumed boundaries and velocity field.

The material enters into the die through Zone I, in which it is still rigid. And it deforms plastically in Zone II which is divided from Zone I with the boundary Γ_2. Plastic deformation stops at the boundary of exit side, Γ_1, Γ_3, Γ_4 and Γ_5 are the inside walls of cylinders, die, and exit channel. Zone III is the region in which the material moves as a rigid body.

and boundaries and Eq. (3) is the formula giving the power, i.e. the energy expensed for a unit of the time, of the work necessary to extrude the material through conical die, in which the yield stress is considered as a function of strain.

$$\begin{aligned} J^* &= \tfrac{2}{3}\int_v \sigma \tfrac{1}{2}\epsilon_{ij}\epsilon_{ij}\,dV + \int_{S_\Gamma} \tau|\Delta v|\,dS \\ &= \pi v_f R_f^2 f(\alpha)\int_0^{\epsilon_f} \sigma(\epsilon)\,d\epsilon - \sqrt{\tfrac{1}{3}}\,\sigma(\epsilon_f)\pi v_f R_f^2\left(\frac{\alpha}{\sin^2\alpha} - \cot\alpha\right) \\ &\quad + \mu\pi v_f R_f^2 \cot\alpha \int_0^{\epsilon_f} \sigma(\epsilon)(1 + \epsilon_f - \epsilon)\,d\epsilon \end{aligned} \tag{3}$$

where $(1/2)\epsilon_{ij}\epsilon_{ij} \equiv (1/2)\ (\epsilon_{ii}^2 + \epsilon_{jj}^2 + \epsilon_{hh}^2) + (\epsilon_{ij}^2 + \epsilon_{jk}^2 + \epsilon_{ki}^2) = (\epsilon_{rr}^2 + \epsilon_{\theta\theta}^2 + \epsilon_{\psi\psi}^2) + \epsilon_{r\theta}^2$; ϵ_{rr}, $\epsilon_{\theta\theta}$, and $\epsilon_{\theta\psi}$ are the velocity of strain tensor elements, σ and τ are for the tensile yield stress and shear stress at yield, V, and dV for the volume, and volume element of the material in the die, respectively, S is for the surface area bordering between moving and static region such as die wall, and dS for the element of the surface area, Δv for the velocity increment across the bordering surface, v_f the velocity at the exit of conical part of the die, R_f the radius of the exit, ϵ the true strain of the material, ϵ_f

the true strain at the exit, the taper angle, and μ is for the frictional coefficient between the material and the die wall. The function $f(\alpha)$ depends only on the taper angle of the die as Eq. (4).

$$f(\alpha) = \frac{1}{\sin^2\alpha}\left[1 - (\cos\alpha)\sqrt{1 - \tfrac{11}{12}\sin^2\alpha} + \frac{1}{\sqrt{11\times 12}}\, ln \frac{1 + \sqrt{\tfrac{11}{12}}}{\sqrt{\tfrac{11}{12}}\cos\alpha + 1 - \sqrt{\tfrac{11}{12}}\sin^2\alpha}\right] \tag{4}$$

In Eq. (3) von Mises yield criterion, $\tau = \sigma/\sqrt{3}$, is assumed as well as the stress–strain rate law of von Mises. To estimate the frictional forces at the inner surface of the die wall the stress in the direction normal to the wall was calculated with Sachs' equation by neglecting the friction at the wall. The last assumption is self-inconsistent with the fact that the frictional coefficient is now to be determined. However, we use this following after Avitzur as a first approximation.

The pressure necessary to extrude the material in steady-state is obtained by the relation of Eq. (5).

$$P_o = J^*/(\pi v_o R_o^2) \tag{5}$$

where v_o and R_o are the velocity of the material and the radius of the die at the die inlet.

2.3.2 *Formation of dead zone* Formation of immobile layer along the die wall (dead zone formation) was considered by Avitzur. This was done by substituting the last term of Eq. (3) with W_s' of Eq. (6).

$$W_s' = \int_{\Gamma'} \tau \Delta v ds = \sqrt{\tfrac{1}{3}}\pi v_f R_f^2 \cot\alpha' \int_o^{\epsilon_f} \sigma(\epsilon) d\epsilon \tag{6}$$

where α' gives a hypothetical dead zone angle which creates a conical pseudo die wall surface of the same material as is being extruded. The value of α' was determined by trial and error method to minimize the calculated extrusion pressure.

2.4 Distortion pattern of originally square grids

The velocity field assumed in Figure 1 gives the traces of the points which enter to the conical die through Zone I. The method of practice to draw the distortion pattern of the originally square grid and the results of it is also described in detail by Avitzur. We can refer to his description and compare the results of Avitzur with our experimental results and also with the results of slip-line analysis.[2]

3 EXPERIMENTAL

The extruding apparatus of cylinder-piston type, of which the inner diameter of the cylinder was $2R_0 = 10$ mm, was described in the previous papers.[1,2] The molten and quenched polymer was cut by a lathe into a rod-like billet of 10 mm in diameter. The die of cone-shaped hole was used, of which the taper angle, i.e. a half of the vertical angle of the cone, was selected among the values of 10° to 60° and in most of the cases it was 20°. The exit diameters of the dies were $2R_f = 2.0$ to 7.0 mm. The steady-state velocity of extrusion was plotted against the extruding pressure. The pressure above which a steep rise of extrusion velocity was observed, and below which the velocity was negligible, was determined as extrusion pressure. Detailed descriptions of the method of extrusion experiments and the treatment of the data were described in our previous papers.[1,2,6,7] The polymer samples, high density polyethylene, polypropylene, and nylon 6, used in extrusion experiments were characterized as given in Table I.

4 RESULTS AND DISCUSSIONS

4.1 Extrusion pressure and degree of processing

Extrusion pressures plotted against the degree of processing at different temperatures with the die of $\alpha = 20°$ are shown in Figures 2, 3, and 4. Solid lines in the figures indicate the extrusion pressures calculated on the basis of the upper bound theory. Broken lines in the figures show the results of calculation of Eq. (2). The values of coefficient μ used in Eqs. (2) and (3) are listed in Table II. The calculated results of Eqs. (2) and (3) are almost similar to each other, and the agreement between those calculated values and the observed ones are quite good.

4.2 Dependence of extrusion pressures on taper angle α

The results of extrusion experiments by the use of the conical converging dies of various taper angles indicated that the extrusion pressure is dependent on the angle α, as shown in Figure 5 for high density polyethylene Hizex 1200J. In contrast with the observations, the extrusion pressure calculated from Eq. (2), broken lines in Figure 5, showed reverse tendency of decreasing with increasing angle α. The calculated extrusion pressures of Eq. (3) show the tendency of increase with increasing taper angle α above 30°. However, if we take care of the possibility of the formation of the immobile layer along the die wall, i.e. dead zone, lower values of extrusion pressures are estimated, as shown by the use of Eq. (6) in Figure 5 with chain lines. According to the upper bound theorem, the lower the extrusion pressure the more reasonable

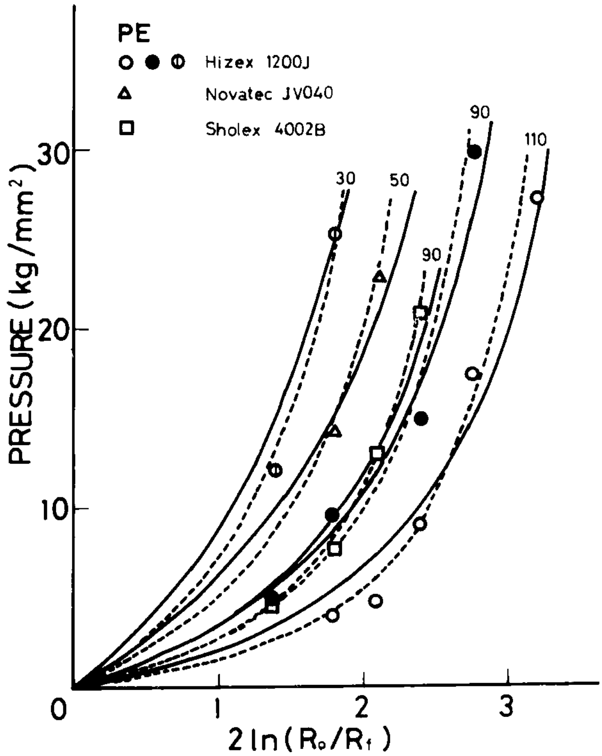

FIGURE 2 Observed and calculated extrusion pressure of high density polyethylene. High density polyethylenes used are distinguished with the symbols given in the figure. The figures on the lines indicate the extrusion temperature. The solid line represents the value calculated with the Eqs. (3) and (5) and the broken line gives the value estimated with Eq. (2). R_0 and R_f are the radius of the cross section of the conical die at the inlet and the exit, respectively.

the assumed velocity field is. Thus, the predicted tendency of decreasing extrusion pressure with increasing taper angle was the same as in the case of the Sachs type equation,[2] Eq. (2), contradicting the observed facts. The real tendency of increasing extrusion pressure with the increasing taper angle was predicted only by the method of slip-line analysis of a flat plane[2] which the precise stress distribution and due complicated velocity field were assumed in including the presence of discontinuities of velocities and their derivatives. In the previous paper,[2] we also examined the effect of the dead zone formation with slip-line method. In that case the formation of dead zones gives no effect on the extrusion pressure. The increase of the extrusion pressure with the change of the longitudinal profile of the die hole is attributable to the change

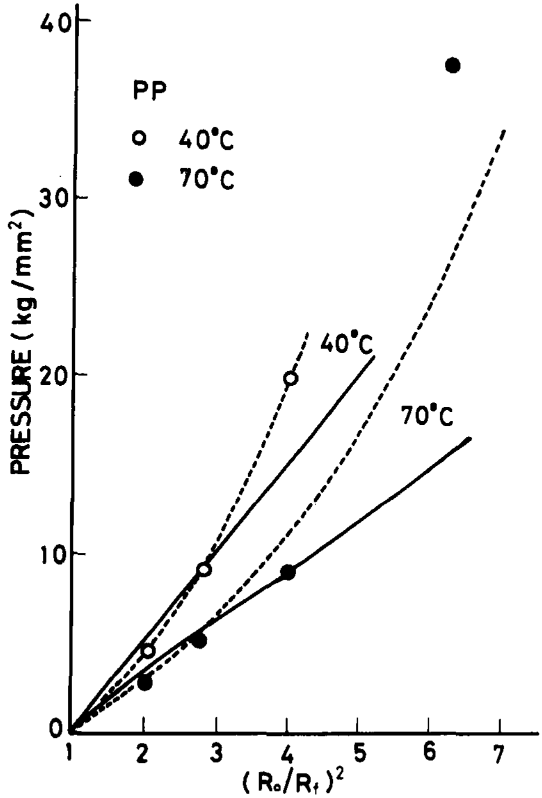

FIGURE 3 Observed and calculated extrusion pressure of isotactic polypropylene. The extrusion temperatures were 40°C (open circles), and 70°C (black circles). The solid lines give the values calculated with the Eqs. (3) and (5). The broken lines give the values calculated with the Eq. (2). The polymer used was Sumitomo-Noblen D501.

of stress, and consequently velocity distribution, especially around the die exit.[2] This conclusion is again confirmed with the fact that no effects of increasing pressure were observed in the upper bound of power on extrusion pressure with changing the die profile, in which the velocity field is continuous and the velocity is simply increasing toward the exit.

4.3 Distortion pattern of originally square grid

The velocity field assumed in Figure 1 is examined by comparing it with that obtained by slip-line analysis. Figure 6 shows the distortion of originally parallel lines calculated from the velocity field of Figure 1. Stream lines, or

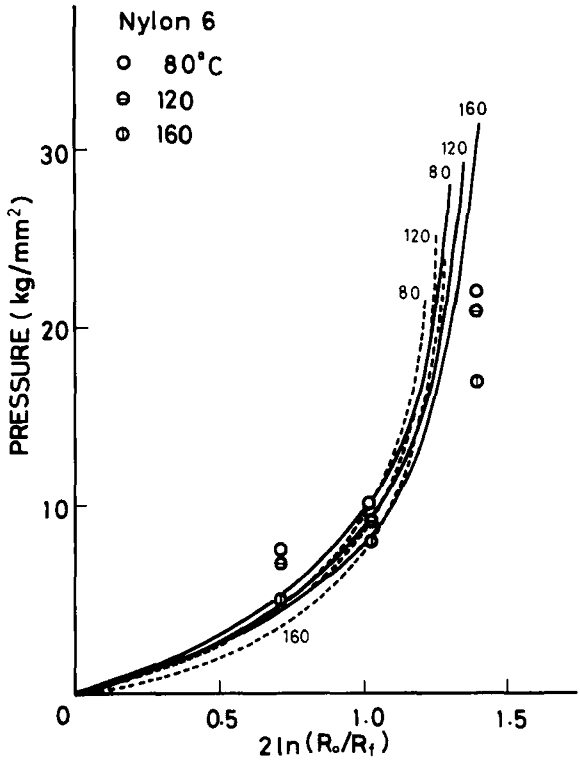

FIGURE 4 Observed and calculated extrusion pressure of nylon 6.
The extrusion temperatures are 80°C, 120° and 160°. The solid lines give the values calculated with the Eqs. (3) and (5), and broken lines those of Eq. (2). The polymer used was Amilan CM1031.

traces of the points progressing toward the exit, are in quite simple arrangement and are omitted from the figure. Those streamlines omitted had been arranged along the central axis in Zone I; as lines of concentric radiation in Zone II; and again along the central axis in Zone III. The stream lines obtained by the slip-line analysis[2] were not arranged as assumed here. Stream lines from the slip-line analysis hang down in the conical region of the die, i.e. the region corresponding to Zone II, toward the central axis as shown in the previous paper.[2] These differences in the arrangement of the stream lines are mainly due to the simplification of the velocity field around the exit of the die. The stream lines obtained by the slip-line method seem to be more realistic.

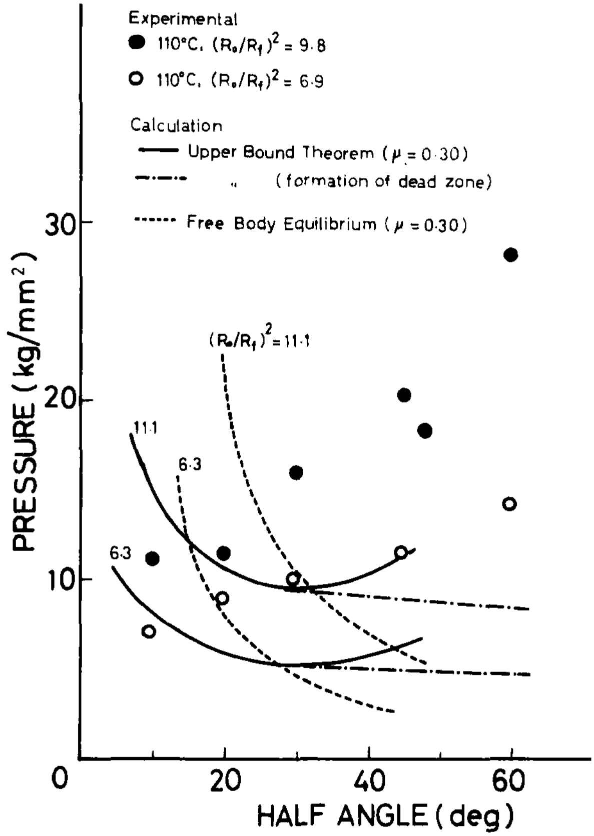

FIGURE 5 Observed and calculated extrusion pressure of high density polyethylene plotted against the angle α.

The extrusion temperature was 110°C, and the ratio of the cross sectional area $(R_0/R_f)^2 = 9.8$ (black circle), and 6.9 (open circle). The solid lines give the values of Eqs. (5) and (3), broken lines those of Eq. (2). The chain lines give the values of the calculation for the case in which the dead zone was formed along the wall of the die, calculated with Eqs. (5), (3) and (6). The polymer used was Hizex 1200J.

The method of the upper bound of power might be useful to examine the adequateness of the analogical stress and velocity field estimation by slip-line analysis in combination with the equation of Sachs type pressure balance. For this purpose, a method of obtaining the power of more complicated and generalized stress and strain rate distribution[8] than that used here is needed.

TABLE II
Frictional coefficient

Polymers	Values of frictional coefficient		
	temperature	μ of Eq. (2)	μ of Eqs. (3) and (5)
High density polyethylene			
Hizex 1200J	30°C	0.23	0.23
	90	0.18	0.23
	110	0.17	0.23
Sholex 4002B	90	0.19	0.23
Novatec JVO40	50	0.22	0.23
Isotactic polypropylene			
Sumitomo-Noblen D501	40	0.30	0.15
	70	0.30	0.17
Nylon 6			
Amilan CM1031	80	0.28	0.15
	120	0.30	0.15
	160	0.36	0.40

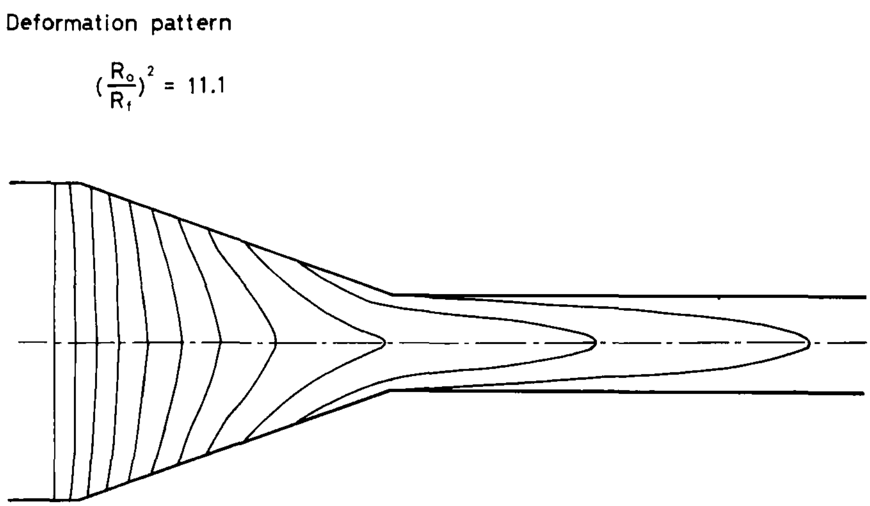

FIGURE 6 The stream lines.
Distortions of the originally parallel lines were calculated with the velocity field assumed as in Figure 1.

References

1. K. Imada, T. Yamamoto, K. Shigematsu, and M. Takayanagi, *J. Mater. Sci.* **6**, 537 (1971).
2. K. Imada and M. Takayanagi, to be published.
3. S. Maruyama, K. Imada, and M. Takayanagi, *Intern. J. Polymeric Mater.* **1**, 211 (1972).
4. B. Avitzur, "Metal Forming Process and Analysis", McGraw-Hill, 1968.
5. W. Prager and P. G. Hodges, Jr., "Theory of Perfectly Plastic Solids", Chapman & Hall Ltd., London, 1951.
6. K. Imada, T. Yamamoto, K. Kanekiyo, and M. Takayanagi, "Mechanical Behavior of Materials", Vol. III, p. 476 (Proceedings of the 1971 Int. Conference on Mechanical Behavior of Mater.), *Soc. Mater. Sci. Jap.* (1972)
7. K. Nakamura, K. Imada, and M. Takayanagi, *Intern. J. Polymeric Mater.* **1**, (1972), in press.
8. Z. Zimerman and B. Avitzur, Trans. *Am. Soc. Mech. Eng.* **B92**, 119 (1970).